

# Recent Advances in the Chemical Synthesis of Lasso Molecular Switches

Frédéric Coutrot

**Abstract** Interlocked and interwoven molecules are intriguing structures that can behave as molecular machines. Among them, the [1]rotaxane molecular architecture is unique, since it defines a lasso-type shape, that, if well designed, can be tightened or loosened depending on an external *stimulus*. This chapter describes an overview of the main strategies used to reach [1]rotaxanes to date and then focuses on the few examples of [1]rotaxanes reported in the literature that behave as mono-lasso or double-lasso molecular machines. Different motions are illustrated like the loosening–tightening of lassos or the controllable molecular “jump rope” movement which is specific to the double-lasso structure.

**Keywords** Molecular machine · [1]Rotaxane · Lasso · Double-lasso · Jump rope · Lasso peptides

## 1 Introduction

Interlocked molecular architectures are the class of compounds that have been extensively studied in the past decades. Rotaxanes and catenanes belong to this family of fascinating compounds: They, respectively, consist of a macrocycle surrounding either a molecular axle or another macrocycle. The number  $[n]$  found in bracket before the chemical terminology “rotaxane” and “catenane” is assigned for the number of elements which are interlocked, without being covalently linked one to each other. It has already been established that the presence of a macrocycle around a thread resulted in tremendous changes of the physical and chemical

---

F. Coutrot (✉)

Supramolecular Machines and Architectures Team, Institut des Biomolécules Max Mousseron, (IBMM) UMR 5247 CNRS-UM1-UM2, Université Montpellier 2, Place Eugène Bataillon, case courrier 1706, 34095 Montpellier Cedex 5, France  
e-mail: frederic.coutrot@univ-montp2.fr  
URL: <http://www.glycorotaxane.fr>

properties of the thread. The same trend has been observed with catenanes, where the properties of a single macrocycle highly differ from the catenated dimer. The fact that the elements of these molecules have the possibility to glide among each other using low interactions gives them very appealing properties. Indeed, not only the new presence of a macrocycle around another element (i.e., a molecular thread in a rotaxane or a macrocycle in the case of a catenane) is responsible for the physical and chemical changes of the element. The different localizations of the macrocycle along the encircled element are also accountable for these changes. As a result, chemists have focused on the design, the synthesis, and the study of numerous molecular machines [1] based on interlocked components which contain several sites of interactions (i.e., molecular stations) for each other. Low interactions between the elements, such as hydrogen bonds, electrostatic, ion–dipole, charge transfer,  $\pi$ – $\pi$  stacking, and hydrophobic interactions, as well as metal-based coordination, have all been utilized to conceive more or less sophisticated molecular stations. Chemical changes such as protonation, deprotonation, photoisomerization, oxidation, reduction, (...) or variations of the environment of interlocked molecular machines such as variations of the solvent, the temperature (...) can lead to the modification of the affinity between the concerned molecular stations and the surrounding macrocycle in rotaxanes and catenanes. Hence, if the molecule is well designed, these changes can cause the controlled displacement of one macrocycle along other components, resulting in the operation of a molecular switch or machine. Among the numerous interlocked molecular architectures reported to date, the lasso compounds hold a particular place, since their constrained looped shape defines a pseudomacrocylic cavity. They can be assimilated to [1]rotaxanes, in which a macrocycle is covalently linked to a molecular tail that threads the macrocycle. Many pseudo[1]rotaxanes have been reported in the literature until now [2–9]: In this typical molecular architecture, an equilibrium takes place between the interlocked compound and its uncomplexed analogue, as long as no bulky moiety is present on the threaded axle (particularly at its extremity) to prevent the disassembling process (Fig. 1). Such compounds that contain both a macrocycle and a site of interaction for it are commonly called “hermaphrodite” molecules.

The synthesis of lasso compounds, in which the interlocked structure is locked at each extremity by two hindering moieties (also commonly called “stoppers”) that prevent the macrocycle to unthread, has been the subject of only a very few report to date. Surprisingly, to the best of our knowledge, only a very small number of lassos have been conceived with the aim of being subjected to molecular machinery. However, the combination of molecular machinery and lariat



**Fig. 1** Cartoon representation of the equilibrium between a pseudo[1]rotaxane and its non-interlocked hermaphrodite analogue

architectures can yield to different movements like those of a belt which can tighten or loosen depending on a pH *stimulus*, or a crank in which a rotational and a translational motions are closely related, or a controllable “jump rope movement” depending on both pH and solvents. In this chapter, attention is first focused on the chemical synthesis of [1]rotaxanes, then on the synthesis and studies of mono-lasso molecular machines, and eventually on the more sophisticated double-lasso molecular machines.

## 2 Main Strategies to Yield Mono-lasso Compounds

Different strategies relative to the synthesis of [1]rotaxanes have been reported in the literature. Whereas most of them involve interactions between sites which are present in both the macrocycle and the axle to be threaded, only one strategy relies on a covalent bond formation of [1]rotaxane devoid from any help of supramolecular interactions. These various main strategies are listed in the following sections.

### 2.1 Covalent Bond Formation of Lasso Compounds

The first strategy to be discussed is based on covalent bond formation and does not appeal to any low interactions between template moieties (Fig. 2). The synthetic route to [1]rotaxanes relies on a key bicyclic compound, one of the two cycles of which can be selectively opened by the attack of a reactive molecular axle (ended by one bulky stopper) through the inner of the other macrocycle.

By using this strategy, Hiratani et al. reported in 2004 the synthesis of the [1]rotaxane **3** via the intermediate formation of the key bicyclic compound **2**, which can undergo an ester to amide *trans*-acylation (Fig. 3) [10].

More precisely, the naphthyl ester moiety of the key bicyclic macrocycle **2** was submitted to an aminolysis using the 9-(3-(aminopropyl)aminocarbonyl)-anthracene. This reaction led, after purification, to the mono-lasso compound **3** in a satisfactory 45 % yield along with 20 % of its non-interlocked analogue. The formation of these two products is inherent in this strategy and can be ascribed to the attack of the amine either by the inner of the cavity of the crown ether or by the

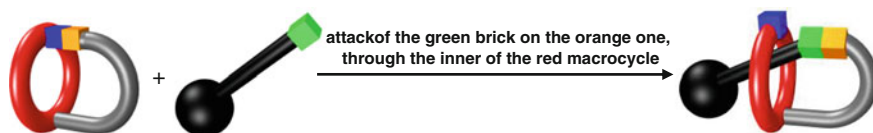
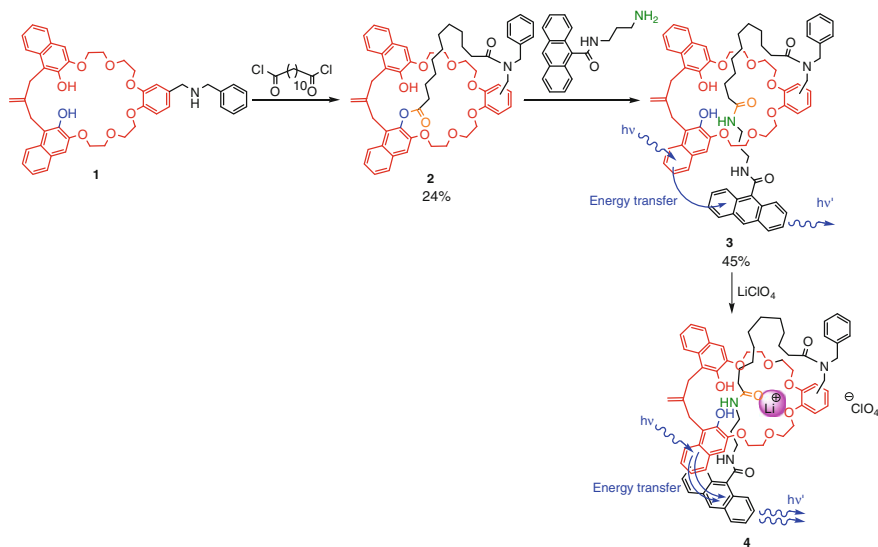


Fig. 2 Cartoon representation of the covalent bond strategy to prepare lasso compounds



**Fig. 3** Covalent bond formation of a lasso compound according to Hiratani et al.

outer of it. Interestingly, and contrary to its non-interlocked analogue, the [1]rotaxane **3** holds specific binding properties related to its interlocked architecture. Indeed, it was found that [1]rotaxane **3** was able to catch the smallest alkali cation lithium with an association constant of  $8.4 \times 10^3 \text{ L mol}^{-1}$ . Energy transfer from the macrocyclic naphthalene to the tail's anthryl group was then observed and studied in the free lasso **3** and in the lithium-complexed lasso **4**. By comparing with **3**, the fluorescence appeared to be enhanced in the case of the lithium-complexed [1]rotaxane **4**, suggesting that the host–guest interactions restrain the conformation of the lasso and decrease the distance between the naphthalene and the anthryl groups, thus lowering the quenching phenomenon.

The other reported strategies to prepare [1]rotaxanes, which are discussed thereafter, are all based on low interactions as the driving force to assemble the molecular elements into the interlocked structure.

## 2.2 Template Synthesis of Lasso Compounds

Three main synthetic template strategies have been utilized to generate lasso compounds (Fig. 4).

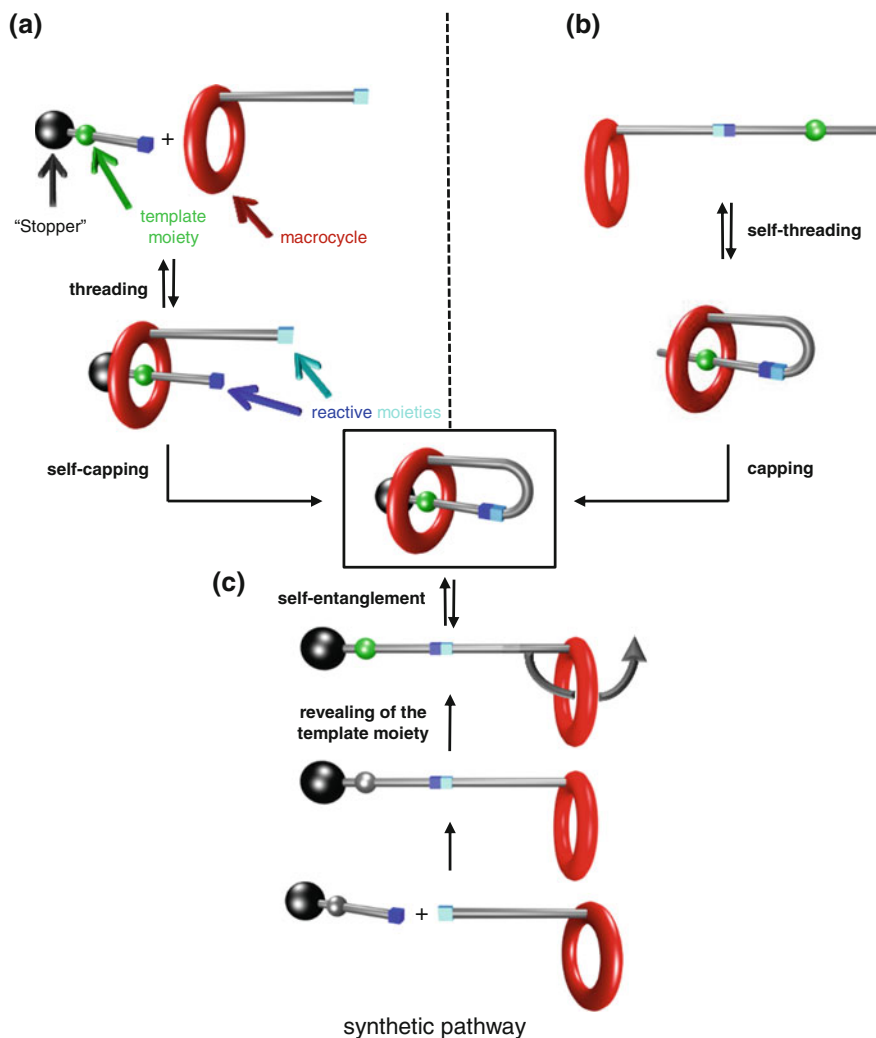


**Fig. 4** Cartoon representation of the three main synthetic template strategies to prepare lasso compounds, **a–c** synthetic pathway

### 2.2.1 Synthetic Pathway (a)

The first synthetic strategy (Fig. 4a) can be divided into two key steps: the preliminary templated synthesis of a semi[2]rotaxane (i.e., a threaded molecular axle that possesses only one bulky stopper) and followed by the chemical connection between two reactive functions which belong to the encircled axle and the surrounding macrocycle.

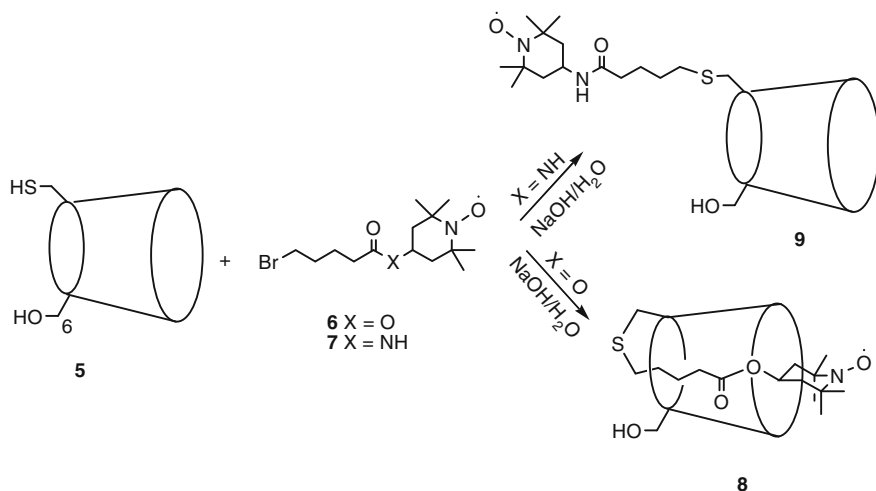


**Fig. 5** Synthesis of a [1]rotaxane based on a cyclodextrin by Lucarini et al.

Using this synthetic pathway, Lucarini et al. reported in 2008 the synthesis of a paramagnetic [1]rotaxane based on a β-cyclodextrin and a nitroxide stopper (Fig. 5) [11]. In water, the 6-mercapto-β-cyclodextrin complexes first the bromide guest compound 6. This encapsulation is due to hydrophobic interactions between 6 and the lipophilic cavity of the cyclodextrin. In the presence of sodium hydroxide, the β-cyclodextrin thiolate moiety of the semirotaxane reacts with the encircled bromide compound via nucleophilic substitution to give the [1]rotaxane 8 in 7.6 % yield. In the case of the bromide compound 7, which contains an amide group, the fortuitous formation of the non-interlocked compound 9 was observed, without any formation of [1]rotaxane. In 8, the 2,2,6,6-tetramethylpiperidine-*N*-oxyl (TEMPO) moiety being larger than the smaller rim of the β-cyclodextrin, it acts as an efficient stopper that locks the structure in a [1]rotaxane molecular architecture.

Due to the stabilization of the nitroxides by the β-cyclodextrin and to the lower reactivity of the nitroxyl group in the [1]rotaxane structure, rotaxane 8 was expected to be more resistant toward the nitroxide reduction carried out by enzymes *in vivo*. Assuming the better *in vivo* stability of nitroxide [1]rotaxane architecture, with respect to non-interlocked nitroxides, such an interlocked structure brings a particular interest for its use as a protected exogenous radical for spin labels, contrast agents for magnetic resonance imaging, the measure of the spectra of a living body, or oximetry, with a stronger and better resolved electron paramagnetic resonance signals.

### 2.2.2 Synthetic Pathway (b)

The second strategy (Fig. 4b) is very similar to the first one, but differs by the fact that the initial threading takes place within a single molecule and firstly affords a

pseudo[1]rotaxane, before that this latter is capped, in a second time, at its threaded extremity. In fact, this strategy can only be envisaged if the starting molecule possesses both a macrocycle and a site of interaction for it. A few number of articles report the synthesis of [1]rotaxanes using this synthetic pathway.

In 2007, Tian et al. reported the synthesis of two  $\beta$ -cyclodextrins-based [1]rotaxanes, in which the cyclodextrins are substituted to a diazo-containing tail at different C6 and C2 positions of the glucidic skeleton (Fig. 6) [12].

In water, the molecules **10** and **13** self-assemble in pseudorotaxanes, through the threading of the diazo moiety in the hydrophobic cavity of the cyclodextrin. Depending on the position of the substitution of the tail on the macrocycle, this threading appeared possible either by the smaller or by the bigger rim of the cyclodextrin. The subsequent end-capping reaction of the pseudorotaxanes was carried out in water using a Suzuki coupling with the boronic acid derivative **11** and afforded the [1]molecular rotaxane architectures.

A very similar [1]rotaxane system has been recently used in the domain of nanomaterials [13]. It involves a  $\beta$ -cyclodextrins-based pseudo[1]rotaxane containing in its molecular tail a diazo moiety for the self-inclusion and a terminal 1,2-dithiolane moiety aimed to be grafted on the surface of gold nanoparticles, these latter acting as the stopper.

The formation of a stable [1]rotaxane without the help of any bulky stopper was reported by Kambe et al. The authors proposed the synthesis of a  $\pi$ -conjugated [1]rotaxane **17** containing a permethylated  $\alpha$ -cyclodextrin which bears a diphenylacetylene derivative (Fig. 7) [14]. Here again, the employed strategy relies on the initial formation of the pseudorotaxane **16** via self-inclusion within a single molecule in a polar medium to enhance the lipophilic interactions, then by the capping reaction of the threaded tail extremity, this time using a Suzuki–Miyaura coupling. In this example, the main novelty lies in the fact that this latter step was achieved using a non-bulky but conjugated stopper. Although the decomplexation through

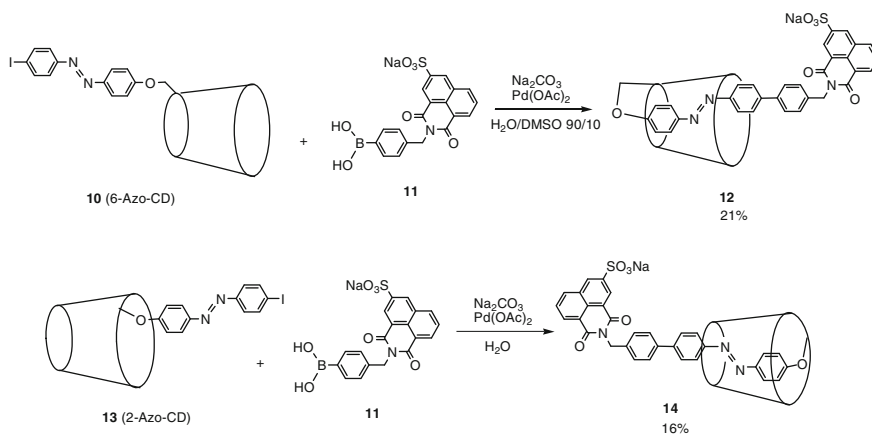


**Fig. 6** Synthesis of a [1]rotaxane based on a  $\beta$ -cyclodextrin by Tian et al.

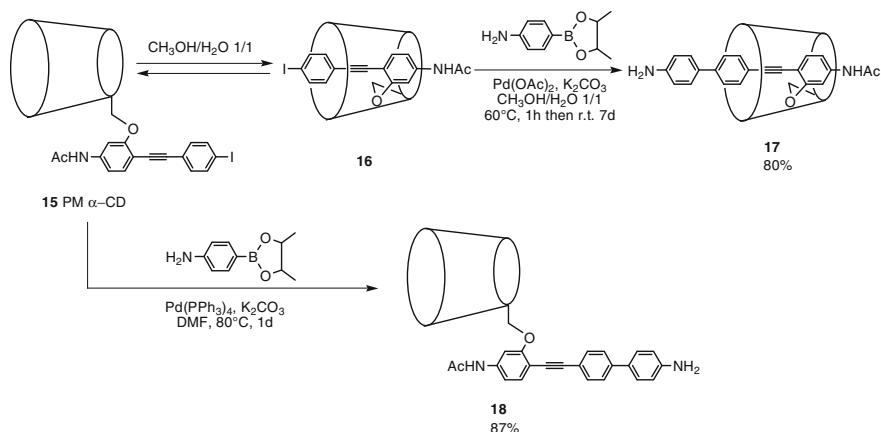


**Fig. 7** Synthesis of a [1]rotaxane based on a permethylated  $\alpha$ -cyclodextrin and using a non-bulky stopper by Kambe et al.

“flipping” of such a flexible permethylated cyclodextrin-based system was already known, here, the [1]rotaxane product appeared very stable in chloroform even after more than seven days. This stability of the interlocked structure **18** can be explained by the rigid  $\pi$ -conjugated aniline moiety which does not allow any “flipping” mechanism.

### 2.2.3 Synthetic Pathway (c)

The third strategy (Fig. 4c) relies first on the synthesis of a macrocycle which is linked to a molecular tail containing already a bulky stopper at its extremity. Contrary to the two first strategies (a) and (b), the absence in the molecular axle of any site of interactions for the macrocycle leads exclusively to the non-interlocked product. However, the revealing of a template moiety for the macrocycle leads to a hermaphrodite molecule, in which the revealed moiety can interact with the macrocycle. In this singular case, the classical threading of the molecular tail extremity is not allowed by the presence of the bulky stopper. Nevertheless, if the aromatic-containing macrocycle is well chosen, in terms of size and substitution [15], a movement of rotation of one of its part authorizes the lasso formation via a reversible self-entanglement process. Due to the reversible process, the obtained lasso belongs to the class of pseudo[1]rotaxanes, as long as the flipping mechanism of the macrocycle is possible. One way to stop this mechanism can be the introduction of a side hindering stopper, located in the tail between the site of interaction and the macrocycle. Another way consists of trapping the interlocked structure using strong interactions like a metal–coordination with ligands located on both the macrocycle and the tail.



In 2010, the synthetic routes (a) and (c) were utilized and compared by Mayer et al. [16] for the preparation of a [1]rotaxane, using a metal-directed complexation as the driving force for the interlocking (Fig. 8).

They proposed the synthesis of a model compound **21**, which contains at one extremity a 31-membered ring holding a 1,10-phenanthroline and a covalently linked molecular axle comprising another phenanthroline moiety. At the other extremity lies a tris(*p-tert*-butylphenyl)methyl group [17], which was already known to be unable to pass through the macrocycle [18, 19]. Compound **21** was synthesized from the two alkene-containing compounds **19** and **20** using the Grubb's metathesis. No interlocked product was generated during the metathesis, which is coherent with the absence of any interactions between the macrocycle and the molecular axle. However, as anteriorly mentioned by Sauvage et al. [20], the addition of copper (I) induces a tetrahedral complex, due to the coordination of the metal with the nitrogen atoms of the two phenanthroline moieties. This complexation forces the structure to adopt the [1]rotaxane molecular architecture **22** by tumbling of the macrocycle. Indeed, since the bulky tris(*p-tert*-butylphenyl)methyl extremity of the molecular axle was chosen so that it cannot thread through the macrocycle, the only way to reach the interlocked structure was demonstrated to be a self-entanglement. This interlocking process was found to be also dependent on concentration. At a high dilution (0.1 mM) that minimizes competitive bimolecular chain-chain complexation, the yield of the rotaxane formation was up to 94 %. The entanglement process can be reversed by removing the copper (I) via its complexation with cyanide ions, resulting in the disappearance of the phenanthroline-copper tetrahedral complex, hence to the disentanglement of the structure.

The other already discussed sequential synthetic route (a) toward the lasso molecule **22** was also investigated. It first consists in preassembling the compounds **19** and **20** in the presence of the copper (I), using its ability to coordinate the phenanthroline units of each component. The semirotaxane complex **23** was found to be very stable and was isolated in 98 % yield before being submitted to the Grubb's metathesis. This afforded the lasso compound **22** in a 77 % yield.

Peculiarly, the various possibilities of internal motion that are inherent to the [1]rotaxane molecular architecture have only been the subject of a very few number of articles that are discussed below.

### 2.3 Examples of Non-controlled Motions in [1]Rotaxanes

An example published by Easton et al. in 2003 [21] must be mentioned as the first synthesized cyclodextrin-based [1]rotaxane. It is based on a cyclodextrin macrocycle and a stilbene-containing thread. The synthetic strategy to reach this [1]rotaxane architecture, which consists of linking the macrocycle of a [2]rotaxane with its encircled axle, has not been discussed before because of its obviousness: Nevertheless, it remains very similar to the presented strategy (a), except that the semi[2]rotaxane is now replaced by a [2]rotaxane. More interesting than the

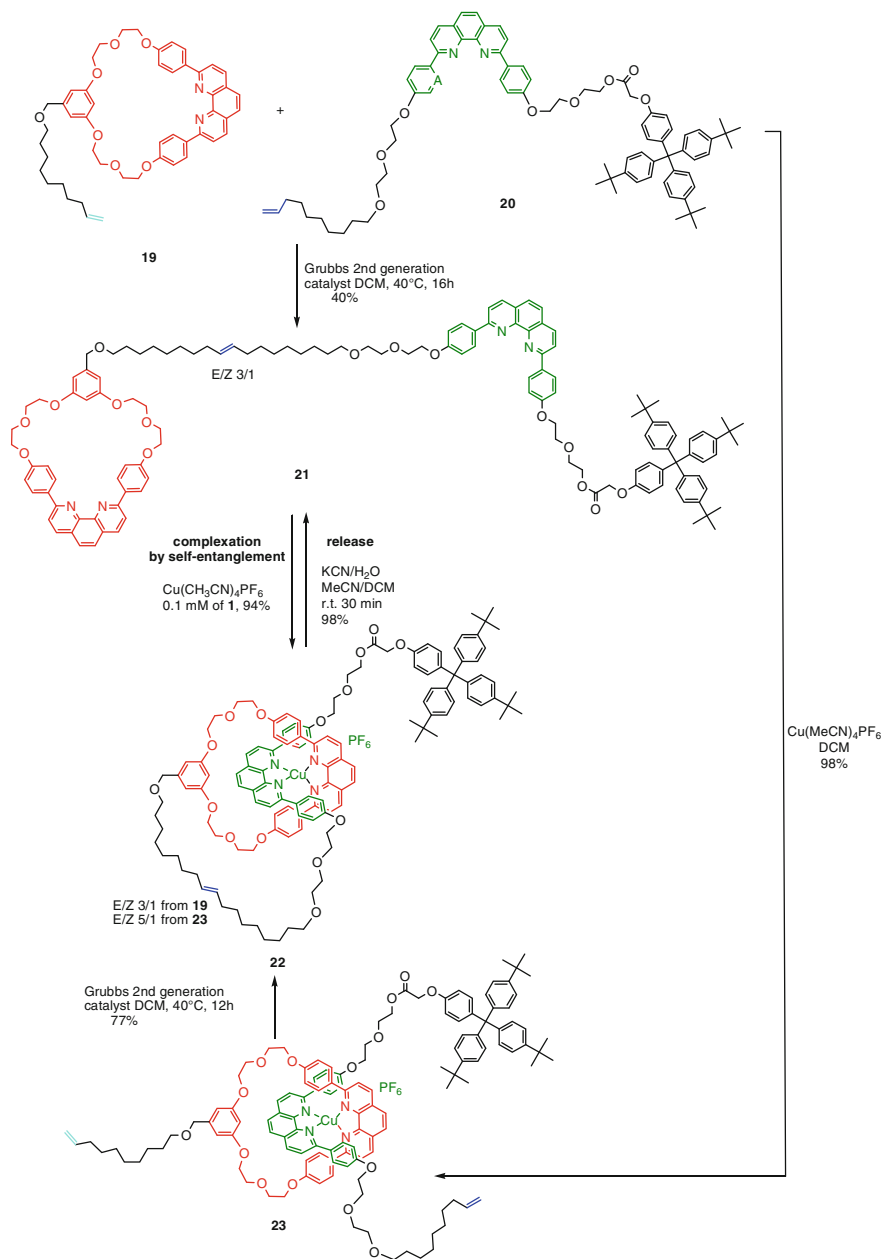


**Fig. 8** Synthesis, capture, and release of a self-entangled [1]rotaxane

synthesis is the study of the rotational motion in a mechanical ratchet of a side part of the encircled thread (i.e., acting as a “tooth”) restricted by the succinamide spacer joining the cyclodextrin and the threaded axle (i.e., acting as a pawl) (Fig. 9). Experiences on a [2]rotaxane analogue, on one hand, and on a similar [1]rotaxane which does not include the methoxy group, on the other hand, proved that this ratchet mechanism is specific to both the [1]rotaxane architecture and the methoxy group.

Another uncontrolled molecular machine was proposed by Shionoya et al. in 2010 [22]. It concerns the design and the synthesis of a molecular “crank” in which an intramolecular motion transformation between rotation and translation can be observed (Fig. 10). The interlocked molecule **26** contains two disk-shaped rotors, each of them linked either to a dibenzo-24-crown-8 (DB24C8) macrocycle or a carbamoylated amine including molecular tail. The whole structure can be assimilated to a [1]rotaxane because the two disk-shaped rotors are linked together via the coordination of three Ag(I) ions, thus joining the DB24C8 macrocycle to the threaded axle. One disk-shaped rotor possesses six monodentate thiazole moieties (in blue), whereas the other contains only three monodentate oxazoline ligands (purple). Both rotors can complex three Ag(I) ions (in green) via the nitrogen atoms of their ligands, and the possibility of exchange between the six thiazole ligands triggers the free rotational movement of one disk shape (the blue one for example)

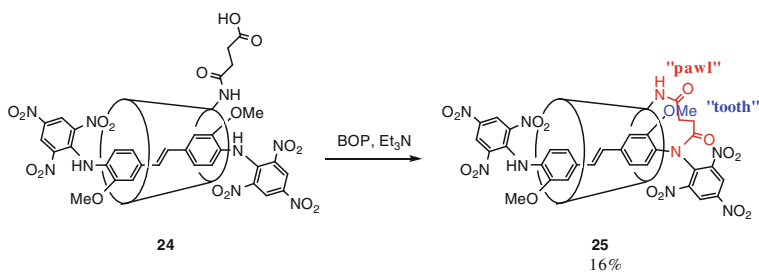
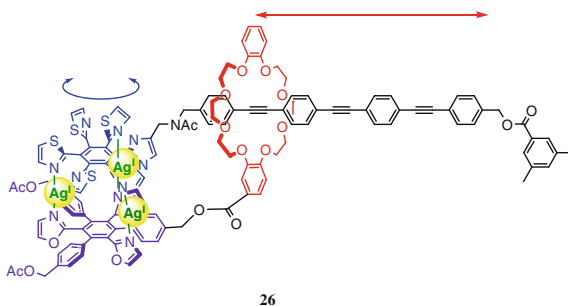


**Fig. 9** A ratchet tooth and pawl to restrict a rotational motion in a cyclodextrin [1]rotaxane by Easter et al.

**Fig. 10** A molecular “crank” by Shionoya et al.



with respect to the other (the purple one). This motion was correlated with the free translational movement of the DB24C8 (in red) along the threaded tail. It is noteworthy that this latter does not contain any molecular station for the DB24C8 in the targeted molecule **26**. Indeed, the initial ammonium moiety, which acts as a necessary template for the interlocking of the molecule during the synthesis, has been carbamoylated so that a free shuttling displacement of the DB24C8 could take place.

These last examples of rotational and rotational related to translational motions naturally lead us to discuss now about the notion of the accurate control of various movements of the elements in a [1]rotaxane. As one of the most interesting internal motion, the molecular machinery of controlling the shuttling of the macrocycle along the thread in a [1]rotaxane architectures has been the object of only a very few examples, which are given below.

### 3 Mono-lasso Molecular Machines

#### 3.1 Synthesis of Light-Driven [1]Rotaxanes

In 2007, Tian et al. described the synthesis of a light-driven [1]rotaxane based on a  $\beta$ -cyclodextrin as the host and a diazo-containing tail as the guest (Fig. 11) [23]. They used the above-discussed strategy (b) consisting of a self-inclusion of an azobenzene-modified  $\beta$ -cyclodextrin and the subsequent tail capping of the pseudorotaxane intermediate by Suzuki coupling. The self-inclusion being mainly based on hydrophobic interactions, the pseudorotaxane **12** was only produced in a

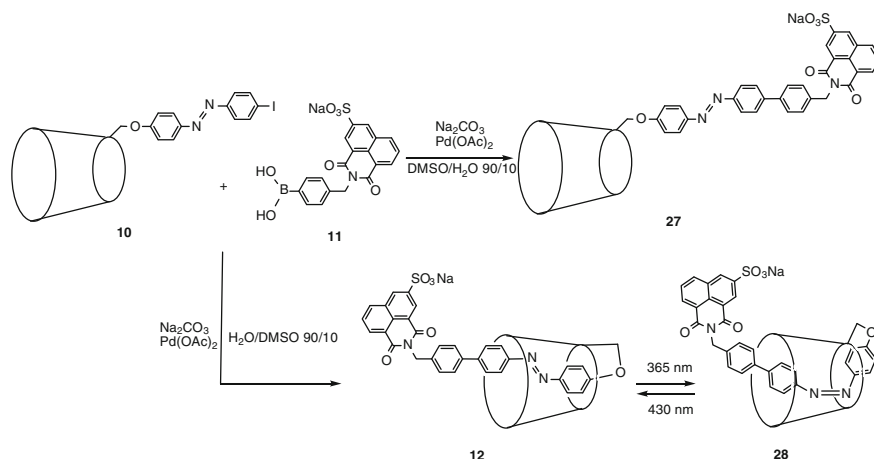


**Fig. 11** Synthesis of a light-driven [1]rotaxane molecular machine based on a cyclodextrin by Tian et al.

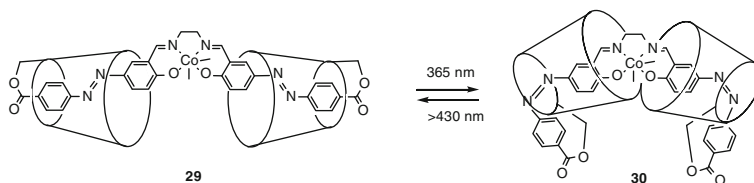


**Fig. 12** Synthesis of a light-driven [1]rotaxane molecular machine by Tian et al.

mixture water/dimethylsulfoxide (90/10), whereas the use of an increased amount of dimethylsulfoxide resulted in the exclusion of the azobenzene arm from the  $\beta$ -cyclodextrin cavity, thus allowing the preparation of the non-interlocked analogue **27**. Interestingly, the *E/Z* photoisomerization of the azobenzene moiety of [1]rotaxanes **12** and **28** triggered a very slight reversible shuttling movement of the  $\beta$ -cyclodextrin along the thread.

Tian et al. reported a little bit later another light-driven [1]rotaxane, this time based on a Cobalt coordinated [1]rotaxane molecular machine which can adopt contracted or stretched states upon light irradiation (Fig. 12) [24]. The Co (III) has been used to coordinate the oxygen atoms of the phenolates and the nitrogen atoms of the Schiff bases, thus allowing a higher rigidity and linearity of the molecule. In **29** and **30**, the photoisomerization of the two azobenzene moieties allows to amplify the stretching and contraction movement that was observed before with the [1]rotaxanes **12** and **28** containing only one azobenzene and one cyclodextrin (Fig. 11).

A few number of other [1]rotaxane molecular machines, this time containing several molecular stations for the macrocycle, have also been recently synthesized and studied. Contrary to the examples described above, they display a much larger amplitude of movement of the macrocycle along the threaded axle, so that the lasso can adopt two very different conformations. They are not based anymore on cyclodextrins but on crown ether macrocycles and have the feature to be pH-responsive. They are inventoried below.

## 3.2 Synthesis of pH-Sensitive [1]Rotaxanes Based on Two Molecular Stations

### 3.2.1 Via the Self-threading and the Subsequent Tail Capping (Synthetic Pathway (b))

All the following examples of lasso molecular machines rely on the utilization of crown ethers as macrocycles and threads containing ammonium and triazolium moieties as molecular stations. Coutrot et al. have been the first to report the use of a *N*-alkyl triazolium as molecular stations [25] for crown ethers such as DB24C8 or

benzometaphenylene-25-crown-8 (BMP25C8). The *N*-methyl triazolium station can be very straightforwardly introduced, from an alkyne and an azide compounds, using a two-step sequence: (1) copper (I)-catalyzed Huisgen alkyne-azide 1,3-dipolar cycloaddition (CuAAC click chemistry) and (2) *N*-methylation of the triazole. The *N*-methyl triazolium moiety proves to be a poorer molecular station for crown ethers than ammonium stations. Indeed, it is quite impossible to use triazoliums as templates for rotaxane formations [26]. However, in interlocked rotaxane architectures, after deprotonation of the ammonium moiety, the *N*-methyltriazolium group turns out to be a molecular station of sufficient affinity for crown ether macrocycles and interacts both by hydrogen bonding or charge transfer.

The bistable ferrocene-based [1]rotaxane **33** was synthesized in 2012 by Qu et al. [27] according to the strategy (b) and using Coutrot's system [25] of molecular stations for the DB24C8 (Fig. 13). The hermaphrodite molecule **31**, which contains an ammonium template linked to a DB24C8 macrocycle via a ferrocene linker, was first synthesized. In the nonpolar solvent dichloromethane, the extremity of the tail is threaded through the macrocycle so that the oxygen atoms of the DB24C8 interact with the ammonium station by hydrogen bonds and ion-dipole interactions. At this stage, the hermaphrodite compound **31** and the pseudorotaxane **32** are in equilibrium. The introduction of a dimethoxybenzene stopper at the alkyne extremity was achieved via the "click chemistry" in a solvent that does

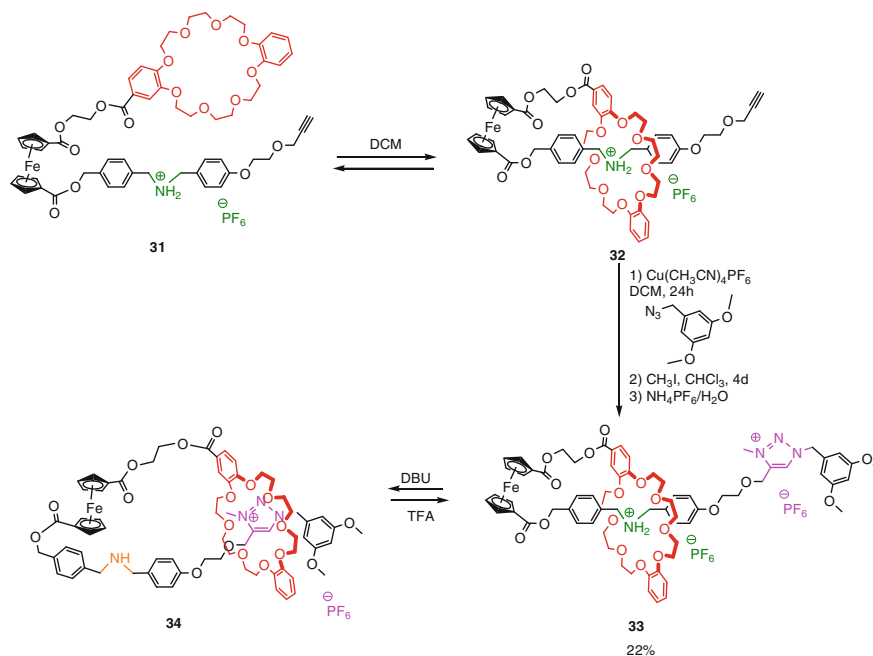


**Fig. 13** Synthesis of a pH-sensitive [1]rotaxane molecular switch with an electrochemical signal output by Qu et al.

not disrupt the interactions that are responsible for the interlocked architecture. Then, the triazole moiety underwent a methylation using methyl iodide and an anion exchange with ammonium hexafluorophosphate. Using Coutrot's synthetic pathway [25], the two-station [1]rotaxane **33** was obtained from the hermaphrodite molecule **31** with an overall yield of 22 %. Molecular machinery was then envisaged on **33** using a variation of pH as the external *stimulus*. Upon deprotonation, the DB24C8 shuttles toward the triazolium station, thus loosening the lasso molecule. The process can be reversed in trifluoroacetic acid, resulting in the tightening of the lasso. Interestingly, cyclic voltammetry experiments showed very different electrochemical properties of the free ferrocene unit for the lasso compounds in the two very different conformational states. Indeed, the electrochemical state of the protonated lasso **33**, in which the ammonium is included in the inner of the macrocycle, appeared reversible. On the contrary, an electrochemically irreversible state is observed at the deprotonated state when the amine group is excluded from the macrocycle. Such a system holds potential for designing smart materials with switchable properties.

Starting from the pseudorotaxane **32** and using the same strategy to yield lasso architecture, Qu et al. described in 2013 an analogous redox-active ferrocene-based system, although slightly more sophisticated insofar as the movement of its DB24C8 displays a larger amplitude and the threaded axle holds a 4-morpholin-naphthalimide as a stopper whose fluorescence can be adjusted by a distance-dependent photoinduced electron transfer process (Fig. 14) [28].

The system works here as an INHIBIT logic gate (Fig. 15) that can be observed by the naked eye. The intensity of the fluorescence of the [1]rotaxanes appeared to be very different depending on the pH. Indeed, by comparing with the protonated [1]rotaxane **35**, the emission intensity at 521 nm of the deprotonated [1]rotaxane **36** dramatically decreases. This observation can be ascribed to the spatial proximity between the electron-rich ferrocene unit and the electron-deficient 4-morpholin-naphthalimide fluorescent moiety. This proximity allows the photoinduced electron transfer process between the two complementary units, thus resulting in the quenching of the fluorescence. Fluorescence can be restored to its original level, either by decreasing the pH (addition of trifluoroacetic acid) or by oxidizing the ferrocene unit by the help of  $\text{Fe}(\text{ClO}_4)_3$ . When oxidized, ferrocene is no more an electron-donating group (compounds **37** and **38**). As a result, no photoinduced electron transfer is possible whatever the distance between the ferrocene and the 4-morpholin-naphthalimide units, this distance being related to the two conformations of the [1]rotaxane which can be obtained upon variation of pH. The authors claimed important potential for the development of complicated logic circuits with memories or sequential functions.

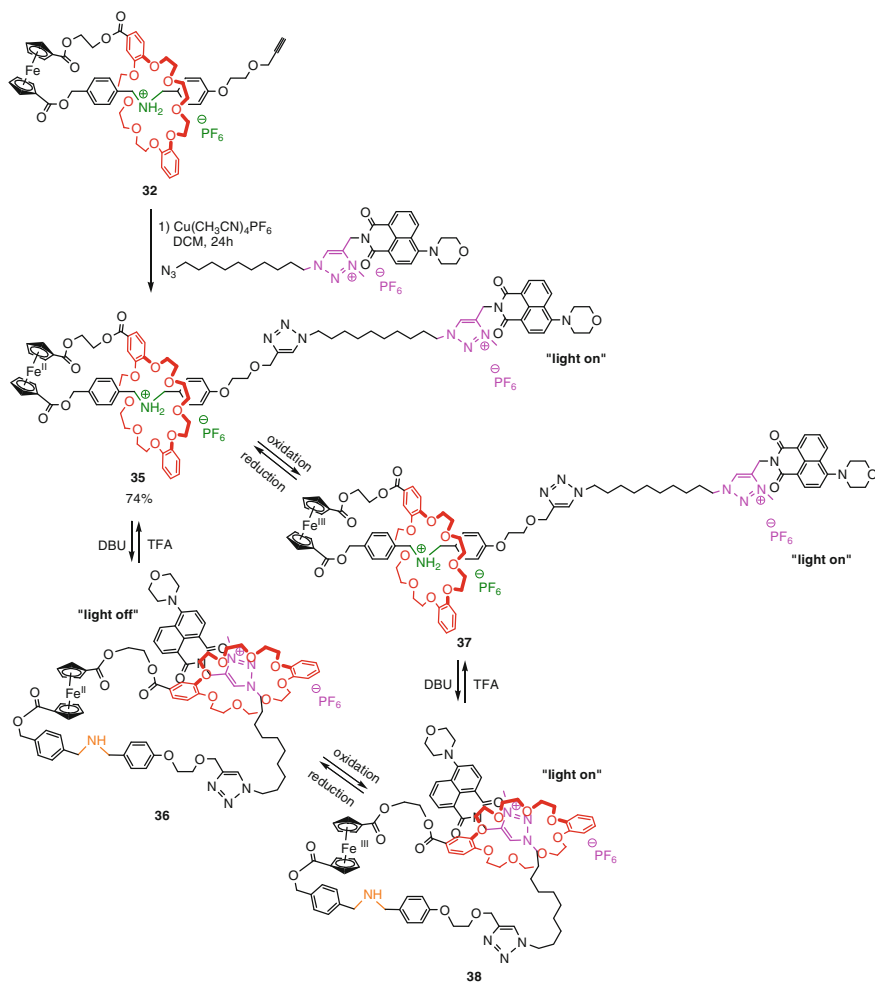


**Fig. 14** Synthesis of a pH-sensitive [1]rotaxane molecular switch holding a fluorescence signal by Qu et al.

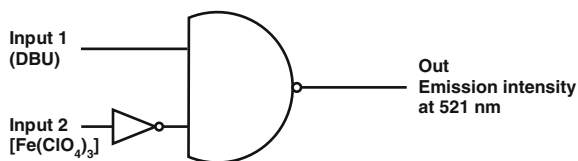


**Fig. 15** Representation of the INHIBIT gate that characterizes the intensity of fluorescence of the [1]rotaxane molecular switches **35–38** upon pH and redox stimuli



### 3.2.2 Via the Self-Entanglement Strategy (Synthetic Pathway (c)) and the Subsequent Introduction of a Kinetic Molecular Barrier

The self-entanglement of a hermaphrodite molecule was recently employed by Coutrot et al. to synthesize two novel [1]rotaxane lasso compounds, which were also able to behave as pH-sensitive molecular switches. The synthetic route to the mono-lasso molecular switches relies here on a two-step sequence: (1) self-entanglement of a hermaphrodite molecule to afford a pseudo[1]rotaxane and (2) trapping of the macrocycle via the incorporation of a kinetic molecular barrier (Fig. 16).

The concept of introducing a molecular barrier to make the molecular machines compartmentalized was developed anteriorly by Leigh et al. [29–33]. Coutrot et al. extended this concept to the *N*-substituted triazolium series, with the aim to use the molecular barrier as a molecular station too [34]. The self-entanglement of the initial hermaphrodite molecule containing a template moiety (green ball) for a macrocyclic host (in red) leads to the pseudo[1]rotaxane, via the rotation of a part of the macrocycle (step 1, Fig. 16). At this stage, the pseudo[1]rotaxane remains in equilibrium with its non-interlocked precursor analogue and can be trapped via the incorporation of a kinetic molecular barrier (pink ball), as a bulky side chain, at a reactive site of the axle located between the template moiety and the macrocycle (step 2, Fig. 16). Bistable molecular machinery on the lasso is then possible only if the threaded axle owns two molecular stations for the macrocycle. In this example, the molecular barrier has been chosen and utilized so that it can also act as a molecular station for the macrocycle, but with a much poorer affinity than the initial template moiety. In the protonated state, the green molecular station has a better affinity for the macrocycle than the pink molecular station, hence resulting in a

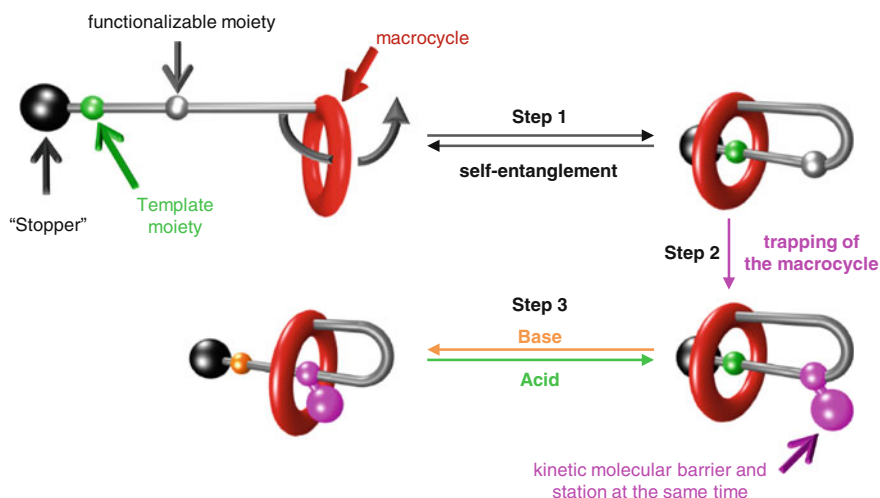


**Fig. 16** Cartoon representation of the self-entanglement and trapping strategy proposed by Coutrot et al.

loosened conformation of the lasso compound. However, deprotonation of the green molecular station triggers the shuttling of the macrocycle toward the pink molecular station, thus causing the tightening of the lasso.

The first targeted mono-lasso has been designed so that the interlocking could be achieved using a template strategy involving hydrogen bonds and ion–dipole interactions between an ammonium moiety and a crown ether macrocycle [35]. The previously prepared hermaphrodite precursor **39u** consists of a benzometaphenylene-25-crown-8 (BMP25C8) macrocycle linked to a molecular axle which contains both an anilinium and a triazole moiety. The anilinium was chosen as the templating site for the crown ether, whether the triazole, which is located between the macrocycle and the anilinium station, has been chosen as the precursor of the triazolium-based molecular barrier and second station.

Since the di-*tert*-butyl anilinium extremity of the molecular axle is too bulky to thread through the macrocycle (i.e., it plays the role of a molecular “stopper”), the only way to yield the lasso architecture relies on the self-entanglement. Thus, the size of the crown ether appears crucial for the efficiency of the pseudo[1]rotaxane formation. Even though a smaller macrocycle such as the dibenzo-24-crown-8 was known to be a better host for the anilinium moiety [36] than the bigger BMP25C8, it could not be utilized in this strategy, due to its smaller cavity (caused by its *ortho*-substitution) that would not allow any self-entanglement. On the contrary, the *meta* substitution of the BMP25C8 enlarges the inner of the macrocycle and allows for the free rotation around the two phenoxy substituting  $\sigma$  bonds of the aromatic ring. This internal movement of the BMP25C8 results in the threading of the anilinium-containing molecular axle by self-entanglement (Fig. 17).

The equilibrium between the uncomplexed hermaphrodite molecule **39u** and the pseudolasso **39** was studied. The pseudolasso was preferentially obtained in hydrogen-bond-promoting solvents and at the lowest concentration. The best self-entanglement (45 % of lasso **39**) was obtained in dichloromethane at a concentration of  $5 \times 10^{-4}$  M, whereas the *ratio* of lasso **39/39u** highly decreased in favor of **39u**, respectively, in acetonitrile (14 % of lasso **39**), methanol (4 % of lasso **39**), and dimethylsulfoxide (0 % of lasso **39**) and upon increasing the concentration in dichloromethane (23 % of lasso **39** at  $5 \times 10^{-2}$  M).

The subsequent trapping of the pseudolasso **39** toward the stable “locked” lasso molecular architecture was realized by benzylation of the triazole moiety (Fig. 18).

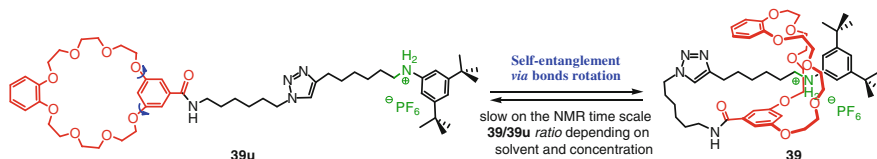


**Fig. 17** Self-entanglement of the hermaphrodite molecule **39u** enclosing a BMP25C8 macrocycle and an anilinium-containing molecular axle by Coutrot et al.

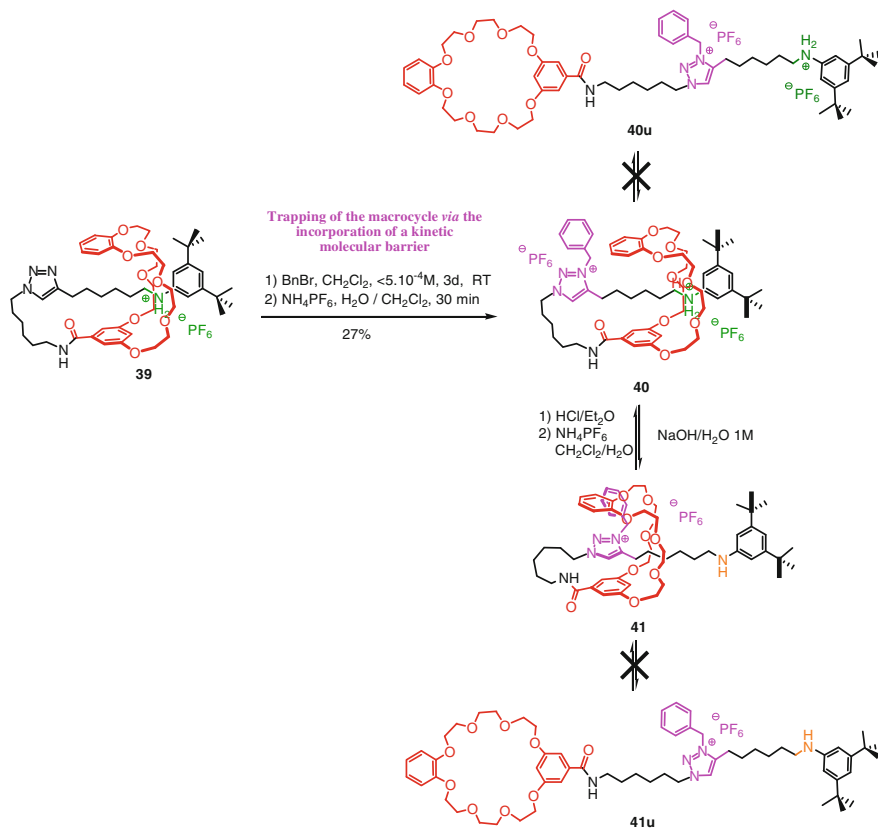


**Fig. 18** Trapping the lasso structure via the *N*-benzylation of the triazole moiety and pH-responsive molecular machinery by Coutrot et al.

The locked [1]rotaxane **40** was isolated in 27 % yield. At this point, the efficacy of the barrier was demonstrated by the absence of any equilibrium between **40** and its uncomplexed hermaphrodite analogue **40u**.

The molecular machinery was then studied, and the evidences were obtained by accurate 1D, 2D, or ROESY  $^1H$  NMR experiments of the protonated and deprotonated lasso molecular switches and of their respective non-interlocked analogues. Deprotonation of the loosened lasso **40** led to the deprotonated tightened lasso **41**, via the shuttling of the BMP25C8 from the anilinium to the triazolium molecular station. Here again, at basic pH, in the absence of the best anilinium station, the benzylic side chain was found to be an effective molecular barrier for the BMP25C8: Indeed, no more equilibrium was observed between the lasso compounds **41** with their respective non-interlocked analogues **41u**.

Inspired by the fact that lasso molecules can also be identified in nature, the same authors pursued their research by trying to give a biological application to synthetic lasso molecular machines. Of particular interest is the case of the different families

of natural lasso peptides, which, for most of them, are resistant against the proteolytic degradation and the chemical and thermal degradation and, for some of them, proved to inhibit the HIV replication or the gram-negative RNA polymerase. Their very interesting biological activities essentially lie on their specific constrained conformation. Their chemical synthesis remains a tough challenge so far, which explains why no lasso peptide has been synthesized using chemical protocols to date. Furthermore, natural lasso peptides are not subjected to molecular machinery, although applying molecular machinery to a lasso peptide could be of very high interest. For example, one may envisage that bending more or less the tridimensional structure of a peptide using *stimuli*-responsive molecular machinery in a lasso structure could result in the tailoring of the activity or affinity of the peptide for, respectively, its enzyme or receptor.

Considering these words, Coutrot et al. reported a variation in the structure of the lasso, by incorporating a tripeptide sequence between the macrocycle and the triazolium molecular station [37]. They opted for the simplest model tripeptide GlyGlyGly and considered if the tightening or the loosening of the lasso could trigger a more or less bent conformation of the peptide sequence (Fig. 19).

It is noteworthy that the peptide moiety did not perturb the self-entanglement strategy or the operation of the molecular machinery which was observed anteriorly on the non-peptide lasso compounds **40/41**. Hence, in the peptide-containing lasso compounds **42** and **43**, the authors proposed that the variation of the pH causes the reversible protonation–deprotonation of the anilinium molecular station, therefore the variation of the shape of the lasso which results in the modification of the peptide shape. Beyond this preliminary and essentially chemical objective, the extension to other peptide sequences of interest is suggested by the authors and could open new avenues to peptide-containing molecular switches with controllable potential medicinal applications.

Few other more sophisticated and unique lasso structures have also been recently reported: They essentially differ from the number of threaded macrocycles. The following section relates the synthesis and the *stimuli*-responsive behavior of double-lasso molecular machines.

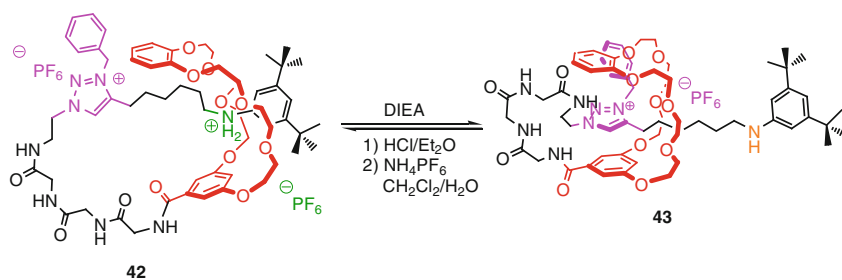


**Fig. 19** Molecular machinery on the pH-sensitive peptide-containing lasso molecular switch **42/43** by Coutrot et al.

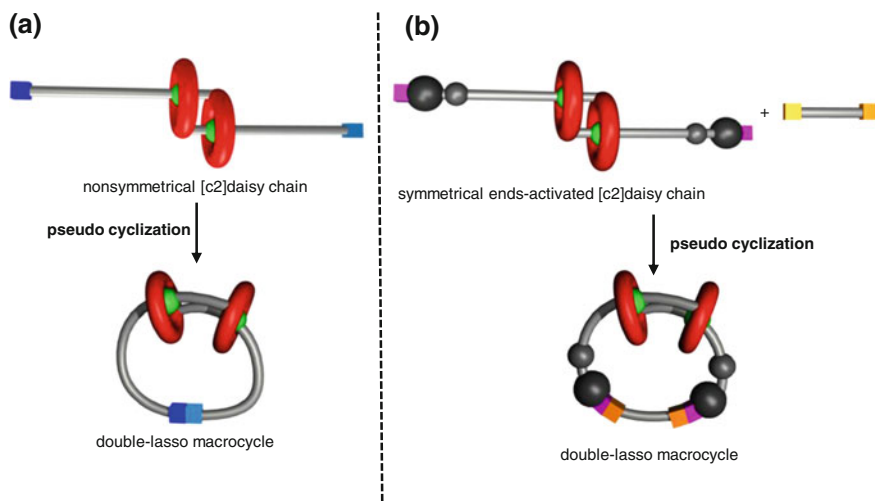


**Fig. 20** Cartoon representation of the two strategies used to prepare double-lasso molecules by the cyclization of [c2]daisy chain precursors by Coutrot et al. **a, b** Synthetic pathway

## 4 Double-lasso Molecular Machines

Two unique double-lasso molecular architectures (Fig. 20) have been recently reported by Coutrot et al. [38, 39]. Their preparation relies on the pseudocyclization of a pseudo[2]rotaxane dimer (i.e., a [c2]daisy chain, for a recent review, see [40]) containing two distinct or identical reactive extremities (Fig. 20). The synthetic pathway (a) involves a self-assembled pseudorotaxane dimer as a key starting material, whereas the other synthetic pathway (b) implies a stable and isolable rotaxane dimer containing two stoppers at each extremity of the interwoven structure.

### 4.1 Synthesis of Double-lasso Macrocycles from Non-symmetrical [c2]Daisy Chain

The first strategy to reach double-lasso macrocycle is essentially based on the preparation of the non-symmetrical [c2]daisy chain enantiomers **49/49'** from two different symmetrical [c2]daisy chains **46** and **48** (Fig. 21) [38].

Analogous but shorter symmetrical dialkyne [c2]daisy chains, based on DB24C8 macrocycles and ammonium station, have been reported by Coutrot et al. anteriorly for the conception of pH-sensitive molecular muscles [41, 42]. In the pseudo[2]rotaxane dimers **49/49'**, the alkyne and azide moieties, which are located at the extremity of the threaded axles, were chosen in order to undergo a copper

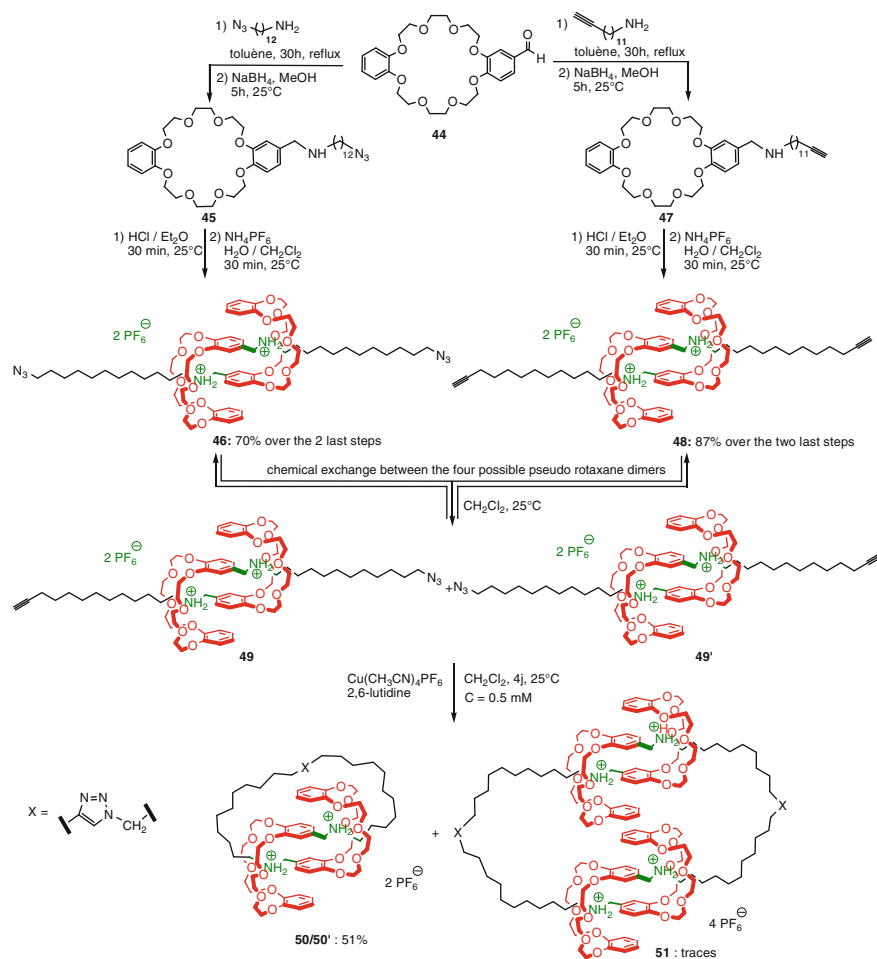


**Fig. 21** Synthesis of the double-lasso macrocycle **50** by Coutrot et al.

(I)-catalyzed Huisgen alkyne-azide 1,3-dipolar cycloaddition (CuAAC click chemistry), thus to create afterward a second molecular station by alkylation of the triazole. They were obtained via the chemical exchange between two different symmetrical diazide and dialkyne [c2]daisy chain precursors **46** and **48**. These latter were produced using a reductive amination reaction from the aldehyde derived from the dibenzo-24-crown-8 **44**.

The necessary exchange between the pseudorotaxane dimers **46** and **48** occurs quickly and leads to the non-symmetrical pseudorotaxane dimer isomers **49/49'**. Contrary to compounds **46** and **48**, and due to the different alkyne and azide extremities, the rotaxane dimer **49** is now devoid of any  $S_2$  symmetry: Therefore, it consists of a stoichiometric mixture of enantiomers. After about 60 min in

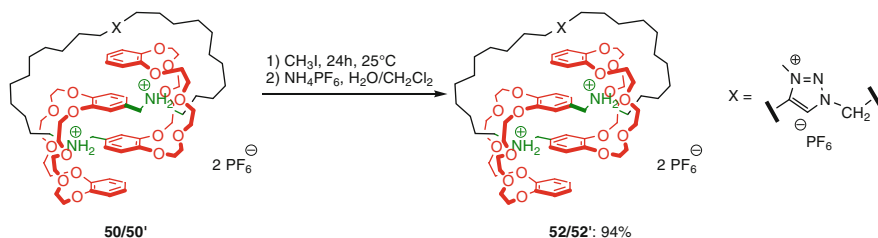


**Fig. 22** Attempt to prepare a double-lasso molecular machine by Coutrot et al.

dichloromethane, the equilibrium was reached and a statistical distribution between **46**, **48**, and **49** was observed by MALDI-TOF mass spectrometry (i.e., **46:48:49/49'** 25:25:50). This observed statistical distribution suggests that the azide or alkyne extremities of each hermaphrodite molecule have no influence on the [c2]daisy self-assembling. The further in situ cyclization of the non-symmetrical pseudorotaxane dimers **49/49'** was carried out and afforded the double-lasso macrocycle **50/50'** in a 51 % yield, which is in concordance with the *ratio* observed for precursors **49/49'**. Only traces of the tetra-lasso macrocycle **51** were detected by MALDI-TOF MS.

The authors then explored the possibility to control the change of the shape of the novel double-lasso structure using molecular machinery. For that, the two triazole moieties were efficiently methylated to create a second molecular station for the DB24C8 macrocycles [43] (Fig. 22).

Unfortunately, neither the deprotonation nor the “one pot” carbamoylation of the ammonium molecular stations led to any reaction that could cause the shuttling of the macrocycles. One may suggest that one triazolium molecular station is not sufficient to bind the two DB24C8 macrocycles.

Another strategy to yield a workable two-station double-lasso molecular machine was envisaged by the authors, this time from a symmetrical ends-activated [c2]daisy chain building block.

## 4.2 Synthesis and Operation of Double-lasso Molecular Machines from a Symmetrical Ends-Activated [c2]Daisy Chain Building Block

### 4.2.1 Synthesis of the Double-lasso Molecular Machines

In this unique example (Fig. 23), the strategy is based on the efficient preliminary synthesis of the [c2]daisy chain building block **54**, which contains at each extremity a bulky protected glucidic stopper [39]. It can be synthesized via the CuAAC click chemistry between the dialkyne [c2]daisy chain **48** and the azido glucuronate active ester **53**. The rotaxane dimer **54** consists of a stable and isolable building block that can react at its extremities via its pentafluorophenyl active ester with amine moieties.

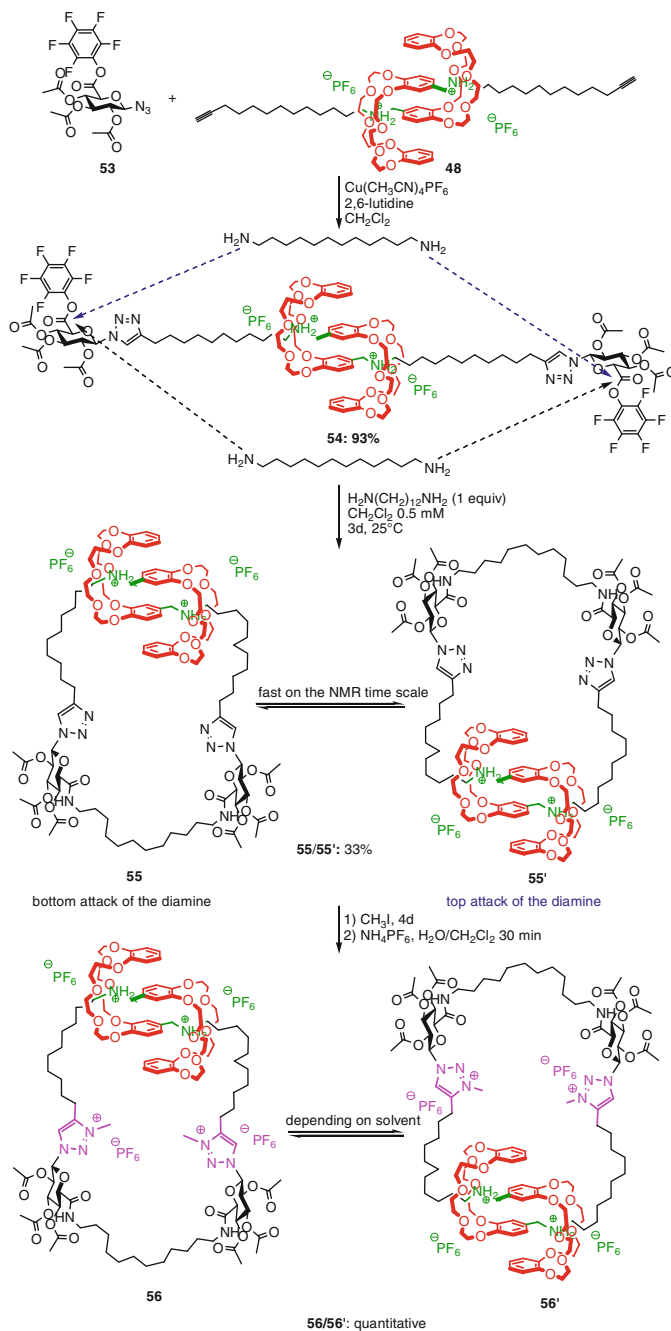


**Fig. 23** Synthesis of a double-lasso molecular machine from an ends-activated [c2]daisy chain building block by Coutrot et al.



Beyond its obvious interest as an elaborated [c2]daisy chain building block for the synthesis of sophisticated pH-responsive polymers, the authors envisaged the formation of double-lasso molecular machines. The pseudocyclization was achieved in dichloromethane at high dilution using the dodecanediamine.

Two possibilities of cyclization are possible here: They are due to the attack of the diamine either by the top of the rotaxane dimer **54**, or by the bottom of it, leading to two double-lasso rotamers **55** and **55'**, that can exchange with each other through the rotation of the pseudomacrocycle around the [c2]daisy arrangement. Since the size of the cavity of the pseudomacrocycle is large enough, the exchange between the two left- and right-handed helix-type rotamers appears fast at the NMR timescale and only one set of  $^1\text{H}$  NMR signal was observed for the two isomers. The *N*-methylation of the triazole moieties was then carried out in order to create the second molecular stations (i.e., the two triazoliums) for the DB24C8 macrocycles.

#### 4.2.2 Tightening and Loosening of the Double-lasso Molecular Machine Triggered by a pH Variation

Contrary to the other previously discussed example of double-lasso molecule **52** which contains only one triazolium site for two macrocycles, the molecular machine appears effective, in the present case, this being ascribed to an equal number of triazolium stations and macrocycles. Indeed, the deprotonation by the sodium hydroxide of the loosened double-lasso **56** triggered the shuttling of the two DB24C8 around the triazolium stations, which led successfully to the tightened double-lasso **57** (Fig. 24) [39].

Lasso **57** proves to be a mixture of isomers, whose exchange is impossible due to the tightened conformation of the lasso (see section below relative to a molecular “jump rope” movement).

Such a molecular machine, which has a cavity of a controllable shape and size, could be of high interest for the future conception of pH-sensitive carriers. If the lasso is well designed in terms of size and nature, one may imagine a guest component confined in the inner cavity of the deprotonated tightened lasso, whereas it is released upon protonation due to the loosening of the lasso that decreases the interactions with the guest molecule.

#### 4.2.3 “Molecular Jump Rope” Motions Dependent on Solvent Polarity and pH

Another distinct movement in the double-lasso molecular machine **56** has also been highlighted. It consists in a controllable rotation (otherwise named a molecular “jump rope” movement) of the loop of the pseudomacrocycle (i.e. the rope) around the [c2]daisy arrangement (i.e., the arms of the girl whose name is Daisy in the cartoon representation illustrated in Fig. 25) [39]. Interestingly, this molecular jump

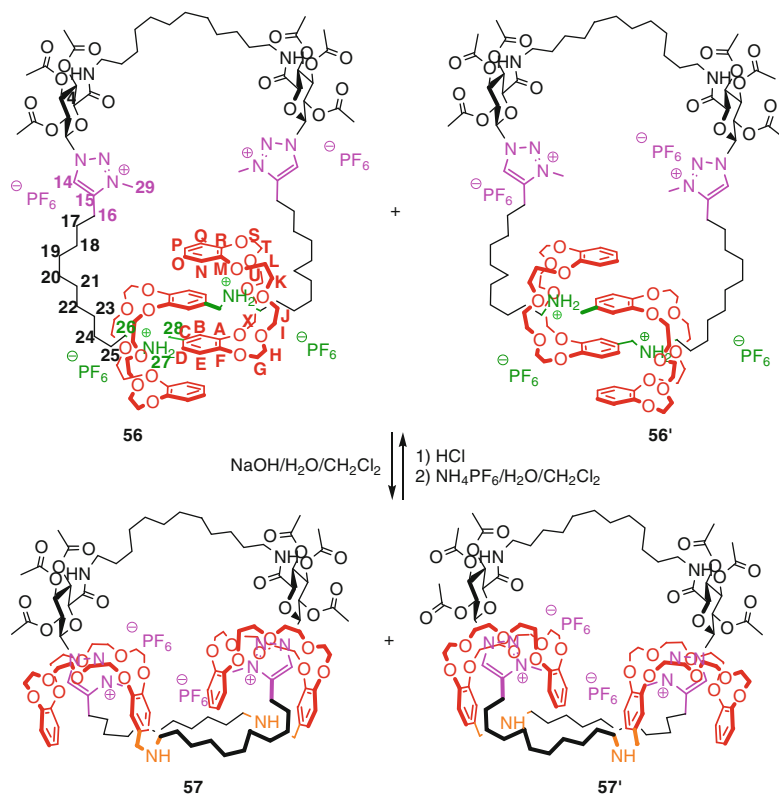


**Fig. 24** Tightening and loosening the double-lasso molecular machine 56/57 upon variation of pH by Coutrot et al.

rope movement could be demonstrated thanks to the <sup>1</sup>H NMR spectroscopy, especially in the case of a slow rotation of the rope, on the NMR timescale, around the daisy arrangement. Indeed, if the rate of the rotation is slow on the NMR timescale, the two rotamers become two atropoisomers (related to D-sugar and left- or right-handed pseudohelices) that are distinguishable by the NMR spectroscopy, like diastereomers. For the triazole-based double-lasso **55**, the exchange between each diastereomer appears to be fast at the NMR timescale, and only one set of signals for **55** is observed. It is not always the case for triazolium-based double-lasso macrocycle **56**. Indeed, the molecular jump rope movement appears here to be solvent-dependent, due to the presence of the triazolium moieties which can be closer or further away from each other, thus lowering or increasing the size of the pseudomacrocycle cavity. In dissociating solvents such as dimethylsulfoxide or acetonitrile, the higher repulsion between the triazolium moieties tends to enlarge the size of the cavity of the rope, allowing a fast movement around the [c2]daisy chain moiety. On the contrary, in the non-dissociating solvent dichloromethane, the repulsion between the triazolium moieties is much smaller, triggering the collapse

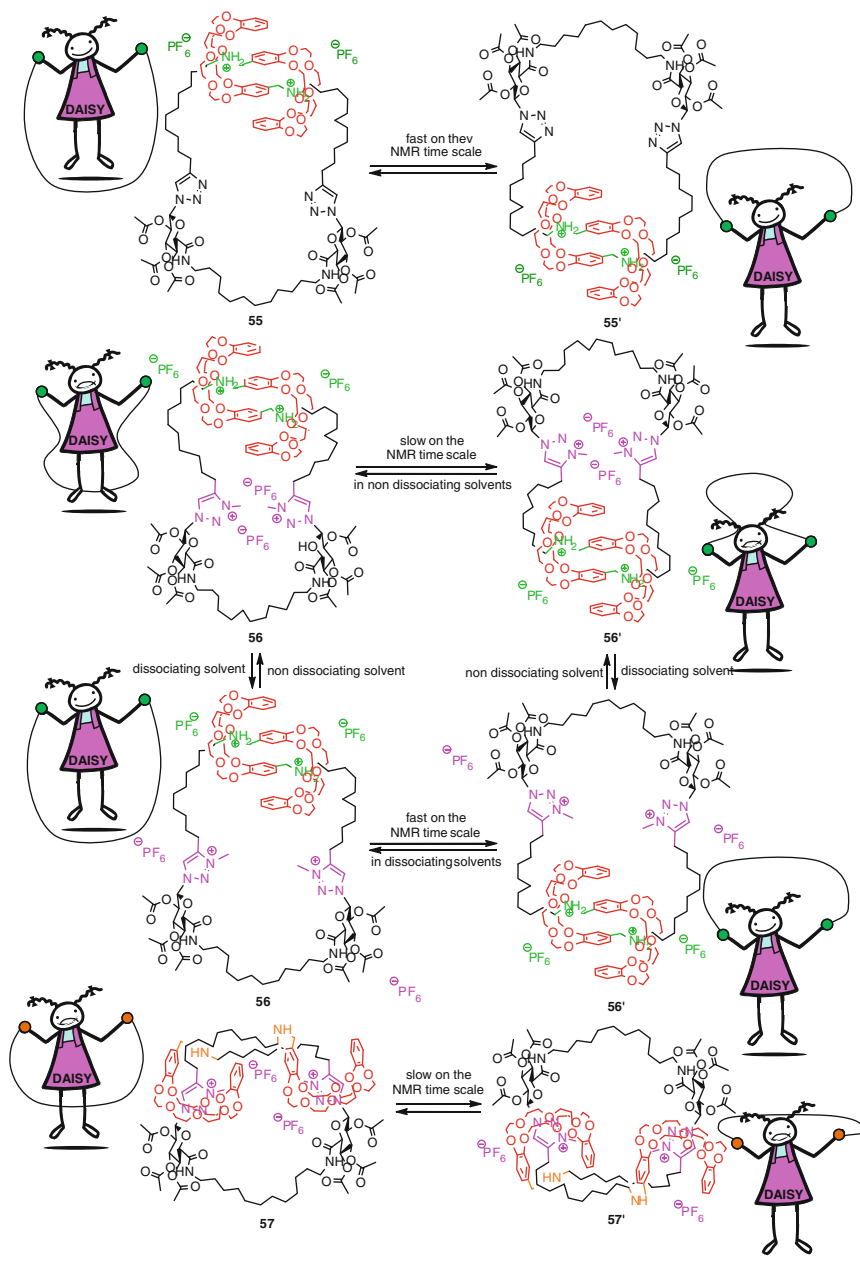


Fig. 25 Molecular "jump rope" movement in double-lasso molecular architectures by Coutrot et al.

of the macrocyclic cavity probably also because of the presence of bifurcated interactions between triazolium cations and hexafluorophosphate counter anions. Hence, the inversion of the helix is hindered in the less polar solvent, and the two rotamers **56** and **56'** are distinguishable by NMR because of the much slower exchange on the NMR timescale. After deprotonation, compounds **57** and **57'** become atropoisomers because the tightening of the double-lasso macrocycle does not permit anymore a free movement of the loop of the lasso around the [c2]daisy chain, then preventing the exchange between the two right- and left-handed helix-type structures.

## 5 Perspectives

Despite the few number of reported papers on [1]rotaxanes, these compounds proved to be very appealing candidates for molecular machinery. Whereas molecular machines based on [2]rotaxane architecture have been studied more extensively, the [1]rotaxanes hold the same opportunity to act as molecular machines and, in addition, they present several advantages that could give rise to many other applications. Indeed, the difference between the two structures relies on the presence of a linker between the macrocycle and the threaded axle, which defines a pseudomacrocycle. The large-amplitude motion of the macrocycle along the threaded pseudomacrocycle can lead to the tightening or the loosening of the lasso. In these two conformational states, the linker, which can be chosen of very different nature (peptide, saccharide, polyether, and polyaromatic), undergoes different conformational changes: If well designed, the incorporation of a bioactive compound (like a peptide), as the linker, could give rise to very different biological responses (in terms of affinity, and activity) depending on the molecular machinery. This could constitute a new field of investigation for lasso compounds. Another interesting purpose of the next few years could be the utilization of the lasso cavity to host a guest molecule in only one of the two tightened or loosened states. As an example, a drug could be encapsulated by an oligosaccharide-containing lasso only at the loosened state, whereas the *stimulus*-dependent tightened conformation would trigger the releasing of the drug as one could squeeze a sponge to extract a substance. By comparison with cyclodextrins, which are very often used to deliver drugs, they usually release continuously their guest components: The lasso molecular machinery could significantly increase the qualities of a molecules carrier by programming a wisely release. And last, but not limited to, the cavity of the lasso compounds could be utilized as nanoreactors in order to catalyze various reactions in only one of the different conformations of the cavity. For sure, the lasso compounds have not yet given all their promises.

## References

1. Kay, E.R., Leigh, D.A., Zerbetto, F.: Synthetic molecular motors and mechanical machines. *Angew. Chem. Int. Ed.* **46**, 72–191 (2007)
2. Balzani, V., Ceroni, P., Credi, A., Gomez-Lopez, M., Hamers, C., Stoddart, J.F., Wolf, R.: Controlled dethreading/rethreading of a scorpion-like pseudorotaxane and a related macrobicyclic self-complexing system. *New J. Chem.* **25**, 25–31 (2001)
3. Yamauchi, K., Miyawaki, A., Takashima, Y., Yamaguchi, H., Harada, A.: Switching from *altro- $\alpha$* -cyclodextrin dimer to pseudo [1]rotaxane dimer through tumbling. *Org. Lett.* **12**, 1284–1286 (2010)
4. Yamauchi, K., Miyawaki, A., Takashima, Y., Yamaguchi, H., Harada, A.: A molecular reel: shuttling of a rotor by tumbling of a macrocycle. *J. Org. Chem.* **75**, 1040–1046 (2010)
5. Ashton, P.R., Ballardini, R., Balzani, V., Boyd, S.E., Credi, A., Gandolfi, M.T., Gomez-Lopez, M., Iqbal, S., Philp, D., Preece, J.A., Prodi, L., Ricketts, H.G., Stoddart, J.F., Tolley, M.S., Venturi, M., White, A.J.P., Williams, D.J.: Simple mechanical molecular and supramolecular machines: photochemical and electrochemical control of switching processes. *Chem. Eur. J.* **3**, 152–170 (1997)
6. Strutt, N.L., Zhang, H., Giesener, M.A., Lei, J., Stoddart, J.F.: A self-complexing and self-assembling pillar[5]arene. *Chem. Commun.* **48**, 1647–1649 (2012)
7. Legros V., Vanhaverbeke C., Souard F., Len C., Désiré J.:  $\beta$ -cyclodextrin-glycerol dimers: synthesis and NMR conformational analysis. *Eur. J. Org. Chem.* **2013**, 2583–2590 (2013)
8. Liu, Y., Yang, Z.-X., Chen, Y.: Synthesis and self-assembly behaviors of the azobenzyl modified  $\beta$ -cyclodextrins isomers. *J. Org. Chem.* **73**, 5298–5304 (2008)
9. Miyawaki, A., Kuad, P., Takashima, Y., Yamaguchi, H., Harada, A.: Molecular puzzle ring: pseudo[1]rotaxane from a flexible cyclodextrin derivative. *J. Am. Chem. Soc.* **130**, 17062–17069 (2008)
10. Hiratani, K., Kaneyama, M., Nagawa, Y., Koyama, E., Kanosato, M.: Synthesis of [1]rotaxane via covalent bond formation and its unique fluorescent response by energy transfer in the presence of lithium ion. *J. Am. Chem. Soc.* **126**, 13568–13569 (2004)
11. Franchi, P., Fani, M., Mezzina, E., Lucarini, M.: Increasing the persistency of stable free-radicals: synthesis and characterization of a nitroxide based [1]rotaxane. *Org. Lett.* **10**, 1901–1904 (2008)
12. Ma, X., Wang, Q., Tian, H.: Disparate orientation of [1]rotaxanes. *Tetrahedron Lett.* **48**, 7112–7116 (2007)
13. Zhu, L., Yan, H., Zhao, Y.: Cyclodextrin-based [1]rotaxanes on gold nanoparticles. *Int. J. Mol. Sci.* **13**, 10132–10142 (2012)
14. Tsuda, S., Terao, J., Kambe, N.: Synthesis of an organic-soluble  $\pi$ -conjugated [1]rotaxane. *Chem. Lett.* **38**, 76–77 (2009)
15. Rowan, S.J., Cantrill, S.J., Stoddart, J.F., White, A.J.P., Williams, D.J.: Toward daisy chain polymers: “Wittig exchange” of stoppers in [2]rotaxane monomers. *Org. Lett.* **2**, 759–762 (2000)
16. Xue, Z., Mayer, M.F.: Actuator prototype: capture and release of a self-entangled [1]rotaxane. *J. Am. Chem. Soc.* **132**, 3274–3276 (2010)
17. Gibson, H.W., Lee, S.-H., Engen, P.T., Lecavalier, P., Sze, J., Shen, Y.X., Bheda, M.: New triarylmethyl derivatives: “blocking groups” for rotaxanes and polyrotaxanes. *J. Org. Chem.* **58**, 3748–3756 (1993)
18. Jiménez, M.C., Dietrich-Buchecker, C., Sauvage, J.-P.: Towards synthetic molecular muscles: contraction and stretching of a linear rotaxane dimer. *Angew. Chem. Int. Ed.* **39**, 3284–3287 (2000)
19. Jimenez-Molero, M.C., Dietrich-Buchecker, C., Sauvage, J.-P.: Chemically induced contraction and stretching of a linear rotaxane dimer. *Chem. Eur. J.* **8**, 1456–1466 (2002)
20. Dietrich-Buchecker, C., Sauvage, J.-P., Kern, J.-M.: Templated synthesis of interlocked macrocyclic ligands: the catenands. *J. Am. Chem. Soc.* **106**, 3043–3045 (1984)

21. Onagi, H., Blake, C.J., Easton, C.J., Lincoln, S.F.: Installation of a ratchet tooth and pawl to restrict rotation in a cyclodextrin rotaxane. *Chem. Eur. J.* **9**, 5978–5988 (2003)
22. Okuno, E., Hiraoka, S., Shionoya, M.: A synthetic approach to a molecular crank mechanism: toward intramolecular motion transformation between rotation and translation. *Dalton Trans.* **39**, 4107–4116 (2010)
23. Ma, X., Qu, D., Ji, F., Wang, Q., Zhu, L., Xu, Y., Tian, H.: A light-driven [1]rotaxane via self-complementary and Suzuki-coupling capping. *Chem. Commun.* 1409–1411 (2007)
24. Gao, C., Ma, X., Zhang, Q., Wang, Q., Qu, D., Tian, H.: A light-powered stretch-contraction supramolecular system based on cobalt coordinated [1]rotaxane. *Org. Biomol. Chem.* **9**, 1126–1132 (2011)
25. Coutrot, F., Busseron, E.: A new glycorotaxane molecular machine based on an anilinium and a triazolium station. *Chem. Eur. J.* **14**, 4784–4787 (2008)
26. Chao, S., Romuald, C., Fournel-Marotte, K., Clavel, C., Coutrot, F.: A strategy utilizing a recyclable macrocycle transporter for the efficient synthesis of a triazolium-based [2]rotaxane. *Angew. Chem. Int. Ed.* **53**, 6914–6919 (2014)
27. Li, H., Zhang, H., Zhang, Q., Zhang, Q.-W., Qu, D.: A switchable ferrocene-based [1]rotaxane with an electrochemical signal output. *Org. Lett.* **14**, 5900–5903 (2012)
28. Li, H., Zhang, J.-N., Zhou, W., Zhang, H., Zhang, Q., Qu, D., Tian, H.: Dual-mode operation of a bistable [1]rotaxane with a fluorescent signal. *Org. Lett.* **15**, 3070–3073 (2013)
29. Chatterjee, M.N., Kay, E.R., Leigh, D.A.: Beyond switches: ratcheting a particle energetically uphill with a compartmentalized molecular machine. *J. Am. Chem. Soc.* **128**, 4058–4073 (2006)
30. Alvarez-Pérez, M., Goldup, S.M., Leigh, D.A., Slawin, M.Z.: A chemically-driven molecular information ratchet. *J. Am. Chem. Soc.* **130**, 1836–1838 (2008)
31. Carlone, A., Goldup, S.M., Lebrasseur, N., Leigh, D.A., Wilson, A.: A three-compartment chemically-driven molecular information ratchet. *J. Am. Chem. Soc.* **134**, 8321–8323 (2012)
32. Kay, E.R., Leigh, D.A.: Beyond switches: rotaxane- and catenane-based synthetic molecular motors. *Pure Appl. Chem.* **80**, 17–29 (2012)
33. Leigh, D.A., Zerbetto, F., Kay, E.R.: Synthetic molecular motors and mechanical machines. *Angew. Chem. Int. Ed.* **46**, 72–191 (2007)
34. Busseron, E., Coutrot, F.: *N*-benzyltriazolium as both molecular station and barrier in [2] rotaxane molecular machines. *J. Org. Chem.* **78**, 4099–4106 (2013)
35. Clavel, C., Romuald, C., Brabet, E., Coutrot, F.: A pH-sensitive lasso-based rotaxane molecular switch. *Chem. Eur. J.* **19**, 2982–2989 (2013)
36. Coutrot, F., Busseron, E., Montero, J.-L.: A very efficient synthesis of a mannosyl orthoester [2]rotaxane and mannosidic [2]rotaxanes. *Org. Lett.* **10**, 753–757 (2008)
37. Clavel, C., Fournel-Marotte, K., Coutrot, F.: A pH sensitive peptide-containing lasso molecular switch. *Molecules* **18**, 11553–11575 (2013)
38. Romuald, C., Cazals, G., Enjalbal, C., Coutrot, F.: Straightforward synthesis of a double-lasso macrocycle from a nonsymmetrical [c2]daisy chain. *Org. Lett.* **15**, 184–187 (2013)
39. Romuald, C., Arda, A., Clavel, C., Jiménez-Barbero, J., Coutrot, F.: Tightening or loosening a pH-sensitive double-lasso molecular machine readily synthesized from an ends-activated [c2] daisy chain. *Chem. Sci.* **3**, 1851–1857 (2012)
40. Rotzler J., Mayor M. (2013) Molecular daisy chains. *Chem. Soc. Rev.* **42**, 44–62
41. Coutrot, F., Romuald, C., Busseron, E.: A new dimannosyl[c2]daisy chain molecular machine. *Org. Lett.* **10**, 3741–3744 (2008)
42. Romuald, C., Busseron, E., Coutrot, F.: Very contracted to extended co-conformations with or without oscillations in two- and three-station [c2]daisy chains. *J. Org. Chem.* **75**, 6516–6531 (2010)
43. Romuald, C.: Des muscles moléculaires dans tous leurs états aux noeuds moléculaires à cavité modulable inédite. Thesis, University of Montpellier 2, Montpellier (2011)